

FILE COPY
NO. 2-W

file as:

~~7-11-51~~ 5.1074

NACA - TN - 1871

NACA TN No. 1871

NATIONAL ADVISORY COMMITTEE FOR AERONAUTICS

TECHNICAL NOTE

No. 1871



A MATHEMATICAL THEORY OF PLASTICITY BASED
ON THE CONCEPT OF SLIP

By S. B. Batdorf and Bernard Budiansky

Langley Aeronautical Laboratory
Langley Air Force Base, Va.



Washington

April 1949

~~FILE COPY~~
~~Technical Note~~
~~on the mathematical~~
~~theory of plasticity~~
~~by Batdorf and Budiansky~~
~~Langley Aeronautical Laboratory~~
~~Langley Air Force Base~~
~~Washington, D.C.~~

Reproduced by
**NATIONAL TECHNICAL
INFORMATION SERVICE**
Springfield, Va. 22151

NATIONAL ADVISORY COMMITTEE FOR AERONAUTICS

TECHNICAL NOTE NO. 1871

A MATHEMATICAL THEORY OF PLASTICITY BASED
ON THE CONCEPT OF SLIP

By S. B. Batdorf and Bernard Budiansky

SUMMARY

A theory of plasticity based on the concept of slip is proposed for the relationship between stress and strain for initially isotropic materials in the strain-hardening range. As treated in the present paper, the theory is an extension to polyaxial stress conditions of the conventional uniaxial stress-strain relation, and time-dependent effects, such as creep and stress relaxation, are not considered.

Previously existing theories can in general be classified into two groups, often called theories of plastic deformation and theories of plastic flow. Deformation theories are based on the assumption that for continual loading the state of strain is uniquely determined by the state of stress. Flow theories are based on the assumption that the increment of strain is uniquely determined by the existing stress and the increment of stress. Theories of both types make additional assumptions concerning the orientation of the principal axes of plastic strain or of increment of plastic strain and concerning the nature of loading and unloading.

The theory proposed is of neither the flow nor the deformation type. Its formulation was guided mainly by physical considerations with respect to the assumed mechanism of plastic deformation, namely slip. The new theory makes no use of the assumptions just mentioned in connection with flow and deformation theories; in fact, according to this theory, all these assumptions are wrong.

The new theory is based on the assumption that slip in any direction along parallel planes of any particular orientation in the material gives rise to a plastic shear strain which depends only on the history of the corresponding component of shear stress. The relation between this plastic shear strain and the corresponding stress can be determined from the tensile stress-strain curve. The plastic strain due to any system of applied stresses is then found by considering the history of the component in each direction of the shear stress on each plane of the material, finding the corresponding plastic shear strain, transforming this plastic shear strain into plastic strains in some fixed system of coordinates, and summing over all slip directions and slip plane orientations. A semigraphical method is given for computing in this manner the strains associated with a given stress state.

The theory is shown to give results in better agreement than previously existing theories with data obtained in an experiment in which a cylinder was compressed into the plastic range and then twisted at constant compressive strain. The theory therefore appears promising, but more theoretical and experimental investigations of the characteristic differences between the new theory and previously existing theories are required before the evidence for or against the new theory can be considered conclusive.

INTRODUCTION

A new theory is proposed for the relationship between stress and strain for initially isotropic metals in the strain-hardening range. The theory seeks to predict the plastic strain that would result from the application in any sequence of arbitrary combinations of stress and requires for this purpose only a knowledge of the uniaxial stress-strain relation for the material.

This theory is essentially quite different from the many theories of plasticity that have previously been proposed. It has been recognized (reference 1) that existing theories of plasticity may in general be classified into two types: deformation theories and flow theories. Both types of theory assume that the relation between stress and strain is governed by one law during loading and by another law (the elastic law in incremental form) during unloading. Loading and unloading are defined in terms of the increase or decrease of some rotationally invariant function of the stresses, those most frequently used being the maximum and the octahedral shear stresses. The two types of theory differ chiefly in that deformation theories propose laws giving plastic strain in terms of applied stress; whereas flow theories propose laws giving increments of plastic strain in terms of applied stress and increments of applied stress. Thus, the previous loading history is assumed to have no effect on strain in deformation theories or on increment of strain in flow theories. These basic assumptions appear to be in the nature of plausible postulates made to facilitate the mathematical formulation and subsequent analysis of the various theories rather than physically evident or experimentally verified facts. Moreover, it is characteristic of both flow and deformation theories that the laws are proposed by means of equations having forms that are more or less arbitrary, which therefore introduce additional assumptions of uncertain validity. For example, in theories of plastic flow, the equations proposed are such that the principal axes of stress and of increment of plastic strain are assumed to coincide. On the other hand, deformation theories assume coincidence of the principal axes of stress and plastic strain. Consequently, although considerable difference of opinion exists concerning the relative merits of flow and deformation theories, it is entirely possible that neither type of theory is correct.

The present theory is of neither the flow nor the deformation type. Unlike most theories proposed to date, its formulation was guided mainly by physical considerations with respect to the mechanism of plastic deformation. The present theory involves none of the assumptions just discussed in connection with flow and deformation theories; indeed, according to this theory, all these assumptions are wrong.

This paper presents the essential features of the new theory and seeks to establish its claim to serious consideration by showing its marked superiority to previously existing theories in accounting for the data obtained in one of the more crucial types of plasticity experiment.

SYMBOLS

Ω	solid angle, used to describe orientation of slip planes, steradians
β	angular coordinate giving direction of slip, radians
σ	direct stress
σ_L	direct stress at which plastic deformation begins
τ	shear stress
τ_L	shear stress at which plastic deformation begins
ϵ	total direct strain
ϵ''	plastic strain
γ	total shear strain
γ''	plastic shear strain
x, y, z	rectangular coordinates; used also as subscripts in connection with stress and strain to denote particular components of these quantities
$1, 2$	direction of normal to slip plane and direction of slip, respectively
$F, F(\tau_{12})$	characteristic shear function for material, giving plastic shear strain per steradian of slip-plane orientation per radian of slip direction as a function of shear stress
$l_{x1}, l_{y1}, \dots, l_{z2}$	cosines of angles between x and $1, y$ and $1, \dots$ z and 2 directions

a_n	coefficient of nth term in series expansion for F
$\epsilon_n, \epsilon_n\left(\frac{\sigma}{\sigma_L}\right)$	function giving variation of plastic strain with applied stress in uniaxial compression or tension, corresponding to nth term of series expansion for F
\bar{n}_1, \bar{n}_2	unit vectors in 1 and 2 directions, respectively
$\bar{i}, \bar{j}, \bar{k}$	unit vectors in the x, y, and z directions, respectively
$\bar{m}, \bar{p}, \bar{q}$	unit vectors having directions indicated in figure 8
α, ϕ	polar coordinates used to specify orientation of slip plane (see fig. 8)

ASSUMPTIONS AND LIMITATIONS

The uniaxial stress-strain behavior assumed in the present analysis is the slightly idealized one usually adopted for engineering purposes. The stress-strain curve for first loading is represented by OABC in figure 1. The straight part of this curve OA is called the elastic range, and the point A is called the elastic limit. If the load is removed before the stress exceeds the elastic limit, the material returns to its original state at O, and there is no permanent deformation. If, on the other hand, the stress is increased to the value at point B and then is removed, the stress-strain relationship during the unloading process is that given by the dashed line BO'. The line BO' has the same slope as the line OA so that during the unloading the material behaves elastically except that it has undergone permanent plastic strain given by OO'. Upon subsequent loading, the point representing the state of the material stays on the dashed line until it reaches B and then, as the load further increases, continues along the original path toward C. Additional unloadings and loadings follow the same pattern of unloading along a line parallel to OA and loading along the same line until the stress-strain curve of the original material is reached. At any stage of the loading history just described, the strain may be considered to be the sum of an elastic part related to the stress by Hooke's law and a plastic part determined by the highest value of the stress occurring up to the time under consideration.

The law of plastic deformation to be postulated is in accordance with the uniaxial behavior just described. In its original unstressed state the material is assumed to have identical stress-strain curves in tension and compression. The effect of reversal of loading upon the plastic behavior is not treated in this paper other than to state in passing that the theory is flexible enough to be adapted to materials with a Bauschinger effect. As in the uniaxial case, time-dependent

effects, such as creep, elastic recovery, and the effect on the stress-strain curve of rate of loading, are neglected.

THEORY

Physical considerations.— Slip lines are commonly observed in metals undergoing plastic deformation. On the assumption that, at least for some metals, slip is the principal mechanism of plastic deformation, the present theory was formulated in such a manner as to incorporate the main features of this phenomenon. These features are now reviewed.

When a metal crystal is subjected to a small shear stress, it undergoes elastic shear deformation. (See fig. 2.) As the stress increases beyond a certain limiting value, small blocks of the crystal commence to slide with respect to each other along crystallographic planes called slip planes. As the displacements increase, the shear stress required to produce further deformation also increases. The total shear displacement at any time is the sum of the elastic shear in the crystal blocks and the shear displacement due to slip between neighboring blocks. When the stress is removed, the elastic component vanishes, but the displacements due to slip remain as a plastic strain. The relationship between applied shear stress and total shear strain for repeated loading and unloading is similar to that described for uniaxial tension and illustrated in figure 1. The shear stress required to produce slip is found to be substantially independent of the normal stress and slip occurs only along certain preferred directions in the slip plane. (See reference 2.)

Accordingly, in the theory, the following assumptions are made: Any strain is the sum of an elastic strain and a plastic strain; plastic strain is composed solely of shear deformations due to slip; these shear deformations are uninfluenced by normal pressures; the plastic shear deformation resulting from slip in any direction in a plane of any given orientation depends only upon the history of the component in the direction of slip of the shear stress on this plane; and the total plastic strain is simply the sum of all the slip deformations that have occurred. If the stress history is such that reverse slip does not occur, the dependence on the aforementioned previous history becomes simply a dependence on the highest previous value of the shear-stress component in question.

Mathematical formulation of the theory.— Although a macroscopically isotropic metal is actually an aggregate of tiny crystals, it is customary and convenient to formulate its stress-strain relations as though it were a continuum. Accordingly, instead of considering a small slip along each of a large number of discrete planes, the theory contemplates an infinitesimal plastic shear strain associated with each infinitesimal fraction of the continuum comprising all possible planes.

It is convenient to represent the orientation of a particular plane by the coordinates of the point at which it would be tangent to a hemisphere. The radius to the point of tangency is the normal to the plane. The axis 1 shown in figure 3 is taken in the direction of the normal to the plane, and the axis 2 denotes a particular direction of slip in the plane. An infinitesimal band of planes may be represented by the normals included in the solid angle $d\Omega$, and an infinitesimal band of slip directions may be represented by $d\beta$. The theory postulates that the slip along the planes $d\Omega$, in the increment $d\beta$ of slip directions, produces an infinitesimal plastic shear strain $d\gamma_{12}''$ associated with the 1,2 axes that is given by

$$d\gamma_{12}'' = F(\tau_{12}) d\Omega d\beta \quad (1)$$

where F is a function depending only on the history of τ_{12} , the shear stress in the 2 direction on the plane perpendicular to the 1-axis.

The contribution of this infinitesimal shear strain to the strains in the standard x-, y-, and z-axes is readily written in terms of the direction cosines of the 1-axis and 2-axis. Thus,

$$\left. \begin{aligned} d\epsilon_x'' &= l_{x1} l_{x2} d\gamma_{12}'' \\ d\epsilon_y'' &= l_{y1} l_{y2} d\gamma_{12}'' \\ d\epsilon_z'' &= l_{z1} l_{z2} d\gamma_{12}'' \\ d\gamma_{xy}'' &= (l_{x1} l_{y2} + l_{y1} l_{x2}) d\gamma_{12}'' \\ d\gamma_{xz}'' &= (l_{x1} l_{z2} + l_{z1} l_{x2}) d\gamma_{12}'' \\ d\gamma_{yz}'' &= (l_{y1} l_{z2} + l_{z1} l_{y2}) d\gamma_{12}'' \end{aligned} \right\} \quad (2)$$

In order to find the total plastic strains in the standard axes, the effects of the plastic shear-strain increments must be integrated over all

directions and all planes. Thus,

$$\left. \begin{aligned}
 \epsilon_x^n &= \int_H \int_{-\pi/2}^{\pi/2} F(\tau_{12}) l_{x1} l_{x2} \, d\Omega \, d\beta \\
 &\dots\dots\dots \\
 \gamma_{xy}^n &= \int_H \int_{-\pi/2}^{\pi/2} F(\tau_{12}) (l_{x1} l_{y2} + l_{y1} l_{x2}) \, d\Omega \, d\beta \\
 &\dots\dots\dots
 \end{aligned} \right\} \quad (3)$$

where H denotes the entire hemisphere. (The slip-direction increment is integrated through 180° to include all possible directions only once.)

If the applied stresses are given in the standard coordinate system as $\sigma_x, \sigma_y, \dots, \tau_{yz}$, the shear stress τ_{12} is given by

$$\begin{aligned}
 \tau_{12} &= l_{x1} l_{x2} \sigma_x + l_{y1} l_{y2} \sigma_y + l_{z1} l_{z2} \sigma_z + (l_{x1} l_{y2} + l_{y1} l_{x2}) \tau_{xy} \\
 &+ (l_{x1} l_{z2} + l_{z1} l_{x2}) \tau_{xz} + (l_{y1} l_{z2} + l_{z1} l_{y2}) \tau_{yz}
 \end{aligned} \quad (4)$$

In order to evaluate the total plastic strains as given by equations (3), analytical expressions for the direction cosines must be used. Appendix A contains such expressions in a system of spherical coordinates.

Characteristic shear function.— It follows from the previous discussion concerning slip that, if τ_{12} is gradually increased, the function F must remain zero until a limiting value τ_L is reached. This limiting value is evidently equal to one-half the elastic limit σ_L in pure tension (or compression) since in a tension test the maximum shear stress is one-half the applied uniaxial stress. Beyond this value, F varies with τ_{12} in a manner characteristic of the material

and is referred to hereinafter as the "characteristic shear function" and the corresponding curve, as the "characteristic shear curve." (See fig. 4.)

The characteristic shear curve can be determined from the stress-strain curve for the material in the following manner. The characteristic shear function F is expanded into the series

$$F(\tau_{12}) = \sum_{n=1}^N a_n \left(\frac{\tau_{12}}{\tau_L} - 1 \right)^n \quad (5)$$

which is then substituted into equation (3). The resulting plastic tensile strain can be shown to be given by

$$\epsilon^p = \sum_{n=1}^N a_n g_n \left(\frac{\sigma}{\sigma_L} \right) \quad (6)$$

where the functions g_n do not depend on the material under consideration. A set of these functions for the case $N = 5$ has been evaluated by the method described in appendix B over a range of stress extending up to 1.8 times the elastic limit stress. The results are tabulated in table 1 and are shown graphically in figure 5.

The determination of the characteristic shear function corresponding to a particular stress-strain curve by means of the g -functions is quite simple. Equation (6) is written for σ/σ_L equal to 1.1, 1.25, 1.4, 1.6, and 1.8; table 1 is used to obtain the numerical values of the g -functions at the corresponding strain in each case. This procedure gives five linear algebraic equations for determining the five unknown coefficients a_1, a_2, \dots, a_5 . These values of the coefficients are then substituted into equation (5). If the stress-strain curve is not known to a stress as high as 1.8 times the elastic limit stress, either fewer equations and fewer g -functions or interpolated values of the g -functions must be used.

Application of theory.— Once the characteristic shear curve has been obtained, it is only necessary to apply equations (3) and (4) to obtain the plastic strains resulting from a given sequence of stresses. The τ_{12} used to evaluate F is, as indicated previously, the largest value of this stress which has occurred for each particular choice of directions 1 and 2 during the history of the loading. Because serious difficulty is involved in evaluating the integrals analytically, the use of approximate methods is advisable. Appendix C describes a semi-graphical method of evaluating the required integrals for any plane-stress condition. The method provides a straightforward procedure for

the calculation of strains with accuracy sufficient for engineering purposes.

COMPARISON WITH EXPERIMENTAL DATA AND DISCUSSION

In most of the experiments that have been performed to test theories of plasticity, the ratios and directions of the principal stresses have been constant throughout the loading. In general, such experiments fail to distinguish sharply between the various theories, and in particular do not provide any basis for choosing between flow and deformation theories (references 3 and 4).

A more crucial type of experiment was performed by Roger W. Peters and Norris F. Dow at the Langley Laboratory of the NACA. In this experiment, a thin aluminum-alloy cylinder was compressed into the plastic range and, with the compressive strain held constant, was then twisted. During the twisting process, the compressive stress decreased. After a shear stress of nearly 12 ksi had been applied, the shear stress and then the compressive stress were removed.

In order to facilitate comparison between the experimental data and the predictions of various plasticity theories, the experimental stresses were adopted as the prescribed conditions and the corresponding strains were computed. The stress combinations applied during twisting and the resulting plastic compressive strain are shown as solid curves in figure 6. It is evident from the figure that plastic action continued throughout the twisting process. This behavior is contrary to what would be expected on the basis of conventional theories. Consider, for example, the dashed curve representing constant octahedral shear stress in figure 6. The region below this curve corresponds to octahedral shear stresses lower than that at the beginning of twisting, and the region above the curve corresponds to higher values of the octahedral shear stress. Comparison of the stress-history curve and the curve of constant octahedral shear stress shows that the octahedral shear stress was decreasing during the early stages of twisting and did not increase above the highest previous value until the applied shear stress exceeded 8.6 ksi. On the assumption that after unloading, plastic action is not resumed until the highest previous value of the loading function is exceeded, octahedral-shear theories would give zero plastic strain up to a shear stress in excess of 8.6 ksi, and similarly maximum-shear-stress theories would predict zero plastic strain up to a shear stress of about 5 ksi. The present theory, on the other hand, predicts plastic action throughout the twisting process, because even when the maximum shear was decreasing in magnitude, its orientation was being changed and new and unhardened planes were being subjected to high shear stresses.

Figure 7 shows that the present theory is not only qualitatively but also quantitatively in rather satisfactory agreement with the test data, in any event in much better agreement than conventional theories.

The total plastic compressive strains, computed by the present theory at shear stresses of 6.3 ksi and 11.8 ksi, were below the measured values by 6 percent and 9 percent, respectively. As the figure indicates, the present theory predicts an almost constant total compressive strain in agreement with experiment. The octahedral-shear theories would predict the elastic relation up to an applied shear stress of 8.6 ksi and the maximum-shear theories, to an applied shear stress of about 5 ksi. The predictions of these theories at higher applied shear stresses have not been plotted because there appears to be no general agreement as to the proper way to apply them in the case of second loading.

The possibility exists, of course, that new flow or deformation theories might be devised using a new stress invariant that would increase continually during the loading sequence accompanying twisting in the experiment just described, and it might at first be suspected that the theory of the present paper is perhaps a flow or deformation theory employing such a loading criterion. The fact that this is not the case can be seen by considering an experiment in which a state of pure tension in the plastic range is maintained approximately constant in magnitude while being rotated in direction. (See reference 4.) According to both flow and deformation theories, if the magnitude of the pure tension decreases slightly during rotation, no plastic deformation can occur. According to the present theory, however, new and unhardened planes acquire large shear stresses during the rotation, and plastic deformation occurs. Moreover, by definition (reference 5), deformation and flow theories predict the increments of the strains for continual loading on the basis of only the corresponding increments of stress and the state of stress immediately prior to application of the stress increments; whereas the present theory requires for such a computation a knowledge of the entire previous stress history so that the extent and nature of the hardening of each plane can be determined.

CONCLUDING REMARKS

Previously existing mathematical theories of plasticity can generally be classified into two types, often called flow and deformation theories. Both types of theory are constructed largely on the basis of mathematical considerations and involve a number of arbitrary assumptions of uncertain validity. The theory proposed herein is of neither the flow nor the deformation type but constitutes an entirely different approach to the problem of plastic behavior, its formulation being guided mainly by physical considerations with respect to the assumed mechanism of plastic deformation, namely slip.

Test data obtained in one of the more crucial types of plasticity experiment are found to be in decidedly better agreement with the present theory than with previously existing theories. The experimental data

however are not very extensive. Before the new theory can be regarded as established, additional experimental data of the same general type must be obtained, the other characteristic differences between the new theory and other theories of plasticity must be explored both theoretically and experimentally, and the range of stresses and strains within which the theory is reasonably accurate must be determined.

Langley Aeronautical Laboratory
National Advisory Committee for Aeronautics
Langley Air Force Base, Va., February 14, 1949

APPENDIX A

DERIVATION OF TRANSFORMATION EQUATIONS IN SPHERICAL COORDINATES

In order to find the shear stress in a given slip plane due to a set of applied stresses as well as to perform the integrations required to determine the corresponding plastic strain, analytical expressions for certain direction cosines used in the analysis should be obtained. Such expressions are now obtained for a polar-coordinate system in which the z-axis is chosen as the polar axis. Because the plasticity theory under consideration makes use of only two directions - namely, the direction of slip within the slip plane and the normal to the plane - only the cosines of these directions are derived. The corresponding unit vectors \bar{n}_1 and \bar{n}_2 , as well as the unit vectors \bar{i} , \bar{j} , \bar{k} , \bar{m} , \bar{p} , and \bar{q} are identified in figure 8.

The direction cosines l_{x1} , l_{y1} , . . . l_{z2} are simply the components of the unit vectors \bar{n}_1 and \bar{n}_2 in the x, y, and z directions. Thus,

$$\left. \begin{aligned} \bar{n}_1 &= \bar{i}l_{x1} + \bar{j}l_{y1} + \bar{k}l_{z1} \\ \text{and} \\ \bar{n}_2 &= \bar{i}l_{x2} + \bar{j}l_{y2} + \bar{k}l_{z2} \end{aligned} \right\} \quad (A1)$$

This resolution of the vectors may be brought about in a succession of easy stages as follows:

From figure 8

$$\bar{n}_1 = \bar{k} \sin \phi + \bar{p} \cos \phi \quad (A2)$$

$$\bar{p} = \bar{i} \sin \alpha + \bar{j} \cos \alpha \quad (A3)$$

From equations (A2) and (A3)

$$\bar{n}_1 = \bar{i} \sin \alpha \cos \phi + \bar{j} \cos \alpha \cos \phi + \bar{k} \sin \phi \quad (A4)$$

Similarly, from figure 8

$$\bar{n}_2 = \bar{m} \cos \beta - \bar{q} \sin \beta \quad (A5)$$

$$\bar{m} = \bar{k} \cos \phi - \bar{p} \sin \phi \quad (\text{A6})$$

$$\bar{q} = -\bar{i} \cos \alpha + \bar{j} \sin \alpha \quad (\text{A7})$$

From equations (A3), (A5), (A6), and (A7)

$$\begin{aligned} \bar{n}_2 = & \bar{i}(\cos \alpha \sin \beta - \sin \alpha \cos \beta \sin \phi) \\ & + \bar{j}(-\sin \alpha \sin \beta - \cos \alpha \cos \beta \sin \phi) \\ & + \bar{k} \cos \beta \cos \phi \end{aligned} \quad (\text{A8})$$

From equations (A1), (A4), and (A8) the expressions for the direction cosines are identified as follows:

$$\left. \begin{aligned} l_{x1} &= \sin \alpha \cos \phi \\ l_{y1} &= \cos \alpha \cos \phi \\ l_{z1} &= \sin \phi \end{aligned} \right\} \quad (\text{A9})$$

$$\left. \begin{aligned} l_{x2} &= \cos \alpha \sin \beta - \sin \alpha \cos \beta \sin \phi \\ l_{y2} &= -\sin \alpha \sin \beta - \cos \alpha \cos \beta \sin \phi \\ l_{z2} &= \cos \beta \cos \phi \end{aligned} \right\} \quad (\text{A10})$$

Substitution of the values for l_{x1} , l_{y1} , . . . l_{z2} from equations (A9) and (A10) in equations (4) and (2) of the text leads, after some manipulation, to the following results: The component in the direction \bar{n}_2 of the shear stress in the plane normal to \bar{n}_1 due to the application of stresses σ_x , σ_y , . . . τ_{yz} is given by

$$\begin{aligned} \tau_{12} = & \frac{1}{2} \sigma_x (\sin 2\alpha \sin \beta \cos \phi - \sin^2 \alpha \cos \beta \sin 2\phi) \\ & + \frac{1}{2} \sigma_y (-\sin 2\alpha \sin \beta \cos \phi - \cos^2 \alpha \cos \beta \sin 2\phi) \\ & + \frac{1}{2} \sigma_z (\sin 2\phi \cos \beta) \\ & + \tau_{xy} \left(\cos 2\alpha \sin \beta \cos \phi - \frac{1}{2} \sin 2\alpha \cos \beta \sin 2\phi \right) \\ & + \tau_{zx} (\cos \alpha \sin \beta \sin \phi + \sin \alpha \cos \beta \cos 2\phi) \\ & + \tau_{yz} (-\sin \alpha \sin \beta \sin \phi + \cos \alpha \cos \beta \cos 2\phi) \end{aligned} \quad (\text{A11})$$

The increments of strain resulting from the increments of shear deformation in the slip plane $d\gamma_{12}''$ are given by

$$\left. \begin{aligned}
 d\epsilon_x'' &= \frac{1}{2} d\gamma_{12}'' (\sin 2\alpha \sin \beta \cos \phi - \sin^2 \alpha \cos \beta \sin 2\phi) \\
 d\epsilon_y'' &= \frac{1}{2} d\gamma_{12}'' (-\sin 2\alpha \sin \beta \cos \phi - \cos^2 \alpha \cos \beta \sin 2\phi) \\
 d\epsilon_z'' &= \frac{1}{2} d\gamma_{12}'' (\sin 2\phi \cos \beta) \\
 d\gamma_{xy}'' &= d\gamma_{12}'' (\cos 2\alpha \sin \beta \cos \phi - \frac{1}{2} \sin 2\alpha \cos \beta \sin 2\phi) \\
 d\gamma_{xz}'' &= d\gamma_{12}'' (\cos \alpha \sin \beta \sin \phi + \sin \alpha \cos \beta \cos 2\phi) \\
 d\gamma_{yz}'' &= d\gamma_{12}'' (-\sin \alpha \sin \beta \sin \phi + \cos \alpha \cos \beta \cos 2\phi)
 \end{aligned} \right\} (A12)$$

APPENDIX B

DETERMINATION OF CHARACTERISTIC SHEAR FUNCTION

The characteristic shear function for a material may be conveniently determined from the uniaxial stress-strain curve for the material. If the z-axis is the axis along which stress is applied (see fig. 8), equations (3), (A9), and (A10) combine to give for the corresponding plastic strain

$$\epsilon_z = \int_0^{\pi/2} d\phi \int_{-\pi/2}^{\pi/2} d\beta F(\tau_{12}) \frac{1}{2} \cos \beta \sin 2\phi (2\pi \cos \phi) \quad (B1)$$

This integration is performed over the hemisphere in front of the x,y plane and, since axial symmetry exists, $d\Omega$ is taken equal to $2\pi \cos \phi d\phi$.

The characteristic shear function F is expanded into the series

$$F(\tau_{12}) = \sum_{n=1}^N a_n \left(\frac{\tau_{12}}{\tau_L} - 1 \right)^n \quad (B2)$$

for $\tau_{12} \geq \tau_L$. For $\tau_{12} < \tau_L$, the characteristic shear function is zero. Consequently, when the value of F from equation (B2) is substituted into equation (B1) the integration should be carried out only over the regions where $\tau_{12} \geq \tau_L$, or

$$\sigma_z \sin 2\phi \cos \beta > \sigma_L \quad (B3)$$

because for uniaxial tension

$$\tau_{12} = \frac{1}{2} \sigma_z \sin 2\phi \cos \beta \quad (B4)$$

and

$$\tau_L = \frac{\sigma_L}{2} \quad (B5)$$

From the use of equations (B2) to (B4), equation (B1) becomes

$$\epsilon_z = \frac{\pi}{2} \int_{\tilde{\tau}}^{\pi-\tilde{\tau}} \int_{-\tilde{\beta}}^{\tilde{\beta}} \left[\sum_{n=1}^N a_n (s \sin t \cos \beta - 1)^n \sin t \cos \frac{t}{2} \cos \beta \right] d\beta dt \quad (\text{B6})$$

where

$$t = 2\phi$$

$$s = \frac{\sigma_z}{\sigma_L}$$

$$\tilde{\tau} = \sin^{-1} \frac{1}{s}$$

and

$$\tilde{\beta} = \cos^{-1} \frac{1}{s \sin t}$$

The integration with respect to β in equation (B6) can be carried out analytically and leads to the following result:

$$\epsilon_z = \sum_{n=1}^N a_n g_n(s) \quad (\text{B7})$$

where

$$g_n(s) = \pi \int_{\sin^{-1}(\frac{1}{s})}^{\pi - \sin^{-1}(\frac{1}{s})} q_n(s, t) dt \quad (\text{B8})$$

and

$$q_1 = \cos \frac{t}{2} \sin t \left[\frac{1}{2} s \sin t (\tilde{\beta} + \sin \tilde{\beta} \cos \tilde{\beta}) - \sin \tilde{\beta} \right]$$

$$q_2 = \cos \frac{t}{2} \sin t \left[\frac{1}{3} s^2 \sin^2 t \sin \tilde{\beta} (\cos^2 \tilde{\beta} + 2) \right. \\ \left. - s \sin t (\tilde{\beta} + \sin \tilde{\beta} \cos \tilde{\beta}) + \sin \tilde{\beta} \right]$$

$$q_3 = \cos \frac{t}{2} \sin t \left[s \sin t (\tilde{\beta} + \sin \tilde{\beta} \cos \tilde{\beta}) \left(\frac{3}{8} s^2 \sin^2 t + \frac{3}{2} \right) \right. \\ \left. - s^2 \sin^2 t \sin \tilde{\beta} (2 + \cos^2 \tilde{\beta}) - \frac{3}{4} \sin \tilde{\beta} \right]$$

$$q_4 = \cos \frac{t}{2} \sin t \left[s^2 \sin^2 t \sin \tilde{\beta} (2 + \cos^2 \tilde{\beta}) \left(\frac{4}{15} s^2 \sin^2 t + 2 \right) \right. \\ \left. - s \sin t (\tilde{\beta} + \sin \tilde{\beta} \cos \tilde{\beta}) \left(\frac{3}{2} s^2 \sin^2 t + 2 \right) + \frac{1}{5} \sin \tilde{\beta} \right]$$

$$q_5 = \cos \frac{t}{2} \sin t \left[s \sin t (\tilde{\beta} + \sin \tilde{\beta} \cos \tilde{\beta}) \left(\frac{5}{16} s^4 \sin^4 t \right. \right. \\ \left. \left. + \frac{15}{4} s^2 \sin^2 t + \frac{5}{2} \right) - s^2 \sin^2 t \sin \tilde{\beta} (2 + \cos^2 \tilde{\beta}) \left(\frac{4}{3} s^2 \sin^2 t + \frac{10}{3} \right) \right. \\ \left. + \sin \tilde{\beta} \left(\frac{5}{24} s^2 \sin^2 t + \frac{2}{3} \right) \right]$$

(B9)

The integrations in equations (B8) have been carried out numerically for the case $N = 5$ for values of σ_z/σ_L equal to 1.1, 1.25, 1.4, 1.6, and 1.8. The integrations were performed by finding the area under fifth-degree curves passing through the first six and last six points corresponding to 11 values of ϕ at each stress level, seven decimal places being retained during the computations. The results obtained are given in table 1 and are shown graphically in figure 5.

The equation

$$F(\tau_{12}) = \sum_{n=1}^5 a_n \left(\frac{\tau_{12}}{\tau_L} - 1 \right)^n \quad (\text{B10})$$

should give a very close approximation to the characteristic shear function for the material when the values a_1, a_2, \dots, a_5 are chosen to satisfy equation (B7) for the case $N = 5$ at the five stress levels for which the numerical integrations were performed. Except for the errors in the integrations, the characteristic shear function so found would lead to a stress-strain curve fitting the one from which it was derived over the entire elastic range and at the five points in the plastic range already indicated. If desired, of course, less accurate characteristic shear functions can be found with less computation by using fewer g -functions and by fitting the stress-strain curve at fewer points.

APPENDIX C

A METHOD OF DETERMINING PLASTIC STRAINS ASSOCIATED
WITH PLANE STRESS

As indicated in equations (3) of the text, the theory gives plastic strains in terms of triple integrations. Because these integrations would prove quite formidable if treated analytically, consideration has been given to approximate methods. The method now to be described is a semi-graphical one designed to facilitate the computation of plastic strains associated with plane stress.

The system of plane stress is assumed to act in the x, y plane, and the hemisphere on which the directions of the slip-plane normals are measured is taken above the x, z plane. This hemisphere is considered to be divided by lines of constant α and constant ϕ into elements of equal area, the projections of which on the x, y plane are illustrated in figure 9. The elements of area on the front half of the hemisphere are denoted by a system of subscripts as indicated in the figure. The mean coordinates (α_m, ϕ_n) of each element of area were calculated and are listed in table 2.

In order to find the shear stress τ_{12} in the plane tangent to the hemisphere at the point (α_m, ϕ_n) , equation (A11) is written in the form

$$\begin{aligned} \left(\frac{\tau_{12}}{\tau_L} \right)_{mn} &= \frac{\sigma_x}{\sigma_L} (A_{mn} \sin \beta - B_{mn} \cos \beta) \\ &\quad - \frac{\sigma_y}{\sigma_L} (A_{mn} \sin \beta + C_{mn} \cos \beta) \\ &\quad + \frac{\tau_{xy}}{\tau_L} (D_{mn} \sin \beta - E_{mn} \cos \beta) \end{aligned} \quad (C1)$$

where

$$A_{mn} = \sin 2\alpha_m \cos \phi_n \quad (C2)$$

$$B_{mn} = \sin^2 \alpha_m \sin 2\phi_n \quad (C3)$$

$$C_{mn} = \cos^2 \alpha_m \sin 2\phi_n \quad (C4)$$

$$D_{mn} = \cos 2\alpha_m \cos \phi_n \quad (C5)$$

$$E_{mn} = \frac{1}{2} \sin 2\alpha_m \sin 2\phi_n \quad (C6)$$

The numerical values of these coefficients are given in table 3.

The contributions of the plastic shear deformation arising from the slip in planes tangent to the part of the hemisphere in the m,n th element of area to the plastic strains measured in the system of coordinates used to specify the applied stresses are given by a similar reformulation of equations (A12):

$$(d\epsilon_x'')_{mn} = \frac{1}{2}(d\gamma_{12}'')_{mn}(A_{mn} \sin \beta - B_{mn} \cos \beta) \quad (C7)$$

$$(d\epsilon_y'')_{mn} = -\frac{1}{2}(d\gamma_{12}'')_{mn}(A_{mn} \sin \beta + C_{mn} \cos \beta) \quad (C8)$$

$$(d\gamma_{xy}'')_{mn} = (d\gamma_{12}'')_{mn}(D_{mn} \sin \beta - E_{mn} \cos \beta) \quad (C9)$$

Equations (C7) to (C9) make use of the assumption, later to be employed also in applying equation (C1), that all planes tangent to the part of the hemisphere in any rectangular element of area may for computational purposes be regarded as concentrated at the mean coordinates of the element.

The values of the shear-stress component τ_{12} at point (m,n) in the directions $\beta = 0^\circ$ and $\beta = 90^\circ$ are computed by using equations (C1). These components are then plotted at right angles from a common origin, and a circle is drawn through the origin and two ends. (See fig. 10(a).) The diameter drawn from the origin then represents the magnitude and direction of the shear stress in the m,n th plane, and the chords drawn from the origin in other directions represent the components of shear stress in those directions.

A circle is then drawn about the origin with a radius corresponding to the elastic-limit shear stress, as in figure 10(b). According to the theory, shear deformations are associated with each direction in which the shear-stress component exceeds the elastic-limit shear stress, the amount of shear deformation in any direction depending on the amount by which the corresponding shear-stress component exceeds the elastic-limit shear stress.

In summing the contributions in the different directions, only discrete directions separated by 9° , as indicated by radial lines in

figure 10(b), are considered. The shear strain in each of these directions is given by

$$\begin{aligned} (d\gamma_{12})_{mn} &= F [(\tau_{12})_{mn}] d\Omega d\beta \\ &= F [(\tau_{12})_{mn}] \left(\frac{\pi}{200}\right) \left(\frac{\pi}{20}\right) \end{aligned}$$

and is found by using the shear-stress component in that direction and the characteristic shear curve for the material. (See fig. 4.) Reference to equations (C7) to (C9) shows that the products of this strain with $\sin \beta$ and with $\cos \beta$ must then be found. The summation over the various directions of slip (direction 2) may then be carried out; this procedure corresponds to performing the integration over β in equations (3).

The operations of finding the plastic shear deformation in each direction and multiplying the result by $\sin \beta$ or by $\cos \beta$ may conveniently be carried out in a single step by the use of a master chart of the type shown in figure 11. Along each radial direction considered are plotted values of $F \cos \beta$ for the material being used. This chart is simply fitted over figure 10(a), which represents the stress state, and the values of $F \cos \beta$ are read off directly (see fig. 12) and added in order to perform the integration over β . The value of this sum is then multiplied by the appropriate coefficient, determined from equation (C7), (C8), or (C9), and table 3. The values of $F \sin \beta$ may be obtained in the same manner by rotating the master chart through 90° . A different work sheet is used for each point (m,n) at which the shear stress on the tangent plane causes plastic shear deformation. For plane-stress systems symmetry exists between the front and rear halves of the hemisphere; thus, the total plastic strains ϵ_x'' , ϵ_y'' , and γ_{xy}'' are found by adding up the corresponding strains computed on each sheet associated with the front half of the hemisphere and by multiplying by 2.

At first sight this method of integration appears quite formidable because the front of the hemisphere is divided into 200 elements, which would appear to require 200 work sheets. In practice, however, it is found that ordinarily many of the elements (m,n) make no contribution to the plastic deformation. In addition, the symmetry properties of the stress state considered are often such that only a quarter or sometimes only an eighth of the hemisphere needs to be considered.

REFERENCES

1. Prager, William: The Stress-Strain Laws of the Mathematical Theory of Plasticity - A Survey of Recent Progress. Jour. Appl. Mech., vol. 15, no. 3, Sept. 1948, pp. 226-233.
2. Seitz, Frederick: The Physics of Metals. McGraw-Hill Book Co., Inc., 1943, pp. 73-76.
3. Prager, W.: On the Interpretation of Combined Torsion and Tension Tests of Thin-Wall Tubes. NACA TN No. 1501, 1948.
4. Drucker, D. C.: Stress-Strain Relations for Strain Hardening Materials - Discussion and Proposed Experiments. Rep. All-3, Graduate Div. Appl. Math., Brown Univ. (Providence, R. I.), Aug. 1947.
5. Prager, W.: Theory of Plastic Flow versus Theory of Plastic Deformation. Jour. Appl. Phys., vol. 19, no. 6, June 1948, pp. 540-543.

TABLE 1
CALCULATED g -VALUES

$$\left[\epsilon^n \left(\frac{\sigma}{\sigma_L} \right) = \sum a_n g_n \left(\frac{\sigma}{\sigma_L} \right) \right]$$

σ/σ_L	g_1	g_2	g_3	g_4	g_5
1.10	0.0311486	0.0020860	0.0001560	0.0000137	-----
1.25	.1671619	.0281396	.0053115	.0010741	0.0002206
1.40	.3744986	.1004147	.0308275	.0099447	.0033785
1.60	.7211448	.2948256	.1354768	.0651761	.0336644
1.80	1.1965026	.6448685	.3883228	.2487629	.1656213



TABLE 2
MEAN COORDINATES OF ELEMENTS OF AREA

[See fig. 9; $\alpha_m = -\alpha_n$]

m,n	α_m (deg)	ϕ_n (deg)
1	4.5	2.9
2	13.5	8.6
3	22.5	14.5
4	31.5	20.5
5	40.5	26.8
6	49.5	33.4
7	58.5	40.6
8	67.5	48.8
9	76.5	58.6
10	85.5	^a 72.8

^aTaken one-third of way from boundary of triangular element to pole.



TABLE 3

TRANSFORMATION COEFFICIENTS

$$[A_{-m,n} = -A_{mn}; B_{-m,n} = B_{mn}; C_{-m,n} = C_{mn}; D_{11-m,n} = -D_{mn}; D_{-m,n} = D_{mn}; E_{-m,n} = -E_{mn}]$$

		A_{mn}				
$n \backslash m$		1,10	2,9	3,8	4,7	5,6
1		0.156	0.453	0.706	0.890	0.986
2		.155	.449	.699	.880	.976
3		.151	.440	.684	.863	.956
4		.147	.425	.662	.834	.925
5		.140	.405	.631	.795	.882
6		.131	.379	.590	.744	.824
7		.119	.344	.537	.676	.749
8		.103	.299	.466	.587	.651
9		.081	.236	.368	.464	.514
10		.046	.134	.209	.264	.293
$n \backslash m$		5	4	3	2	1
		D_{mn}				

		C_{mn}									
$n \backslash m$		1	2	3	4	5	6	7	8	9	10
1		0.099	0.094	0.085	0.073	0.058	0.042	0.027	0.015	0.005	0.001
2		.295	.281	.253	.216	.172	.125	.081	.043	.016	.002
3		.482	.458	.414	.352	.280	.204	.132	.071	.026	.003
4		.653	.621	.560	.477	.380	.277	.179	.096	.036	.004
5		.800	.761	.687	.585	.465	.339	.220	.118	.044	.005
6		.914	.869	.785	.669	.532	.388	.251	.135	.050	.006
7		.983	.935	.844	.719	.572	.417	.270	.145	.054	.006
8		.985	.937	.846	.721	.573	.418	.271	.145	.054	.006
9		.883	.840	.759	.646	.514	.375	.243	.130	.048	.005
10		.563	.535	.483	.412	.327	.239	.155	.083	.031	.003
$n \backslash m$		10	9	8	7	6	5	4	3	2	1
		B_{mn}									

		E_{mn}				
$n \backslash m$		1,10	2,9	3,8	4,7	5,6
1		0.008	0.023	0.035	0.045	0.049
2		.023	.067	.105	.132	.147
3		.038	.110	.171	.216	.239
4		.051	.149	.232	.292	.324
5		.063	.183	.284	.358	.397
6		.072	.209	.325	.410	.454
7		.077	.225	.350	.441	.489
8		.076	.225	.350	.442	.490
9		.070	.202	.314	.396	.439
10		.044	.129	.200	.252	.280



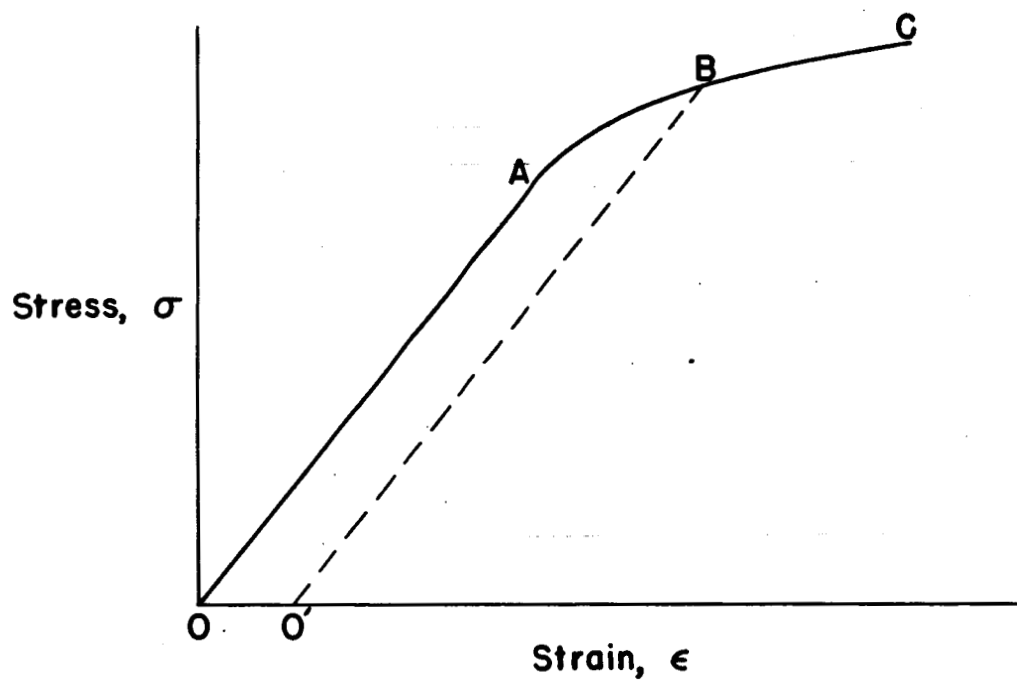


Figure 1. - Uniaxial stress-strain relation.

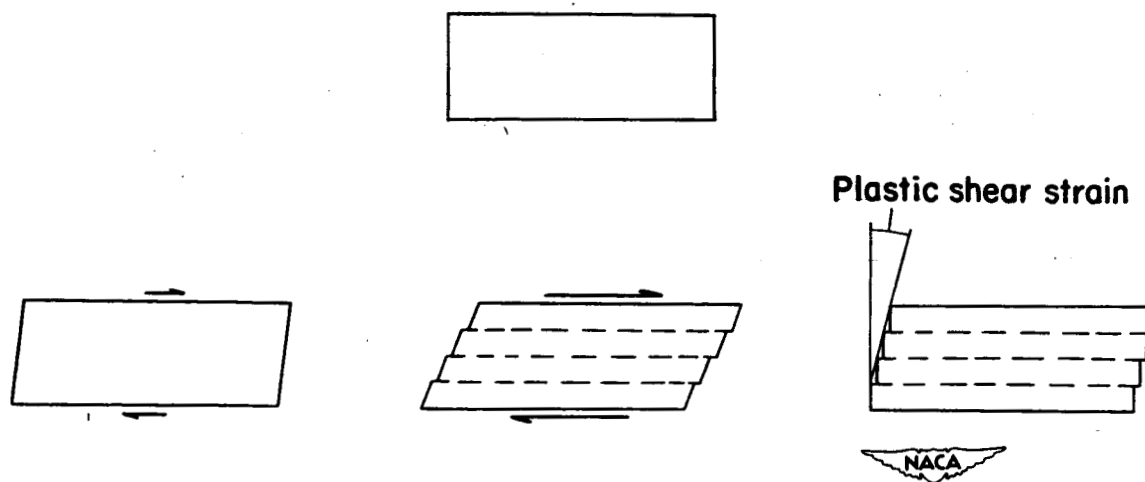


Figure 2. - Slip in single crystal (schematic).

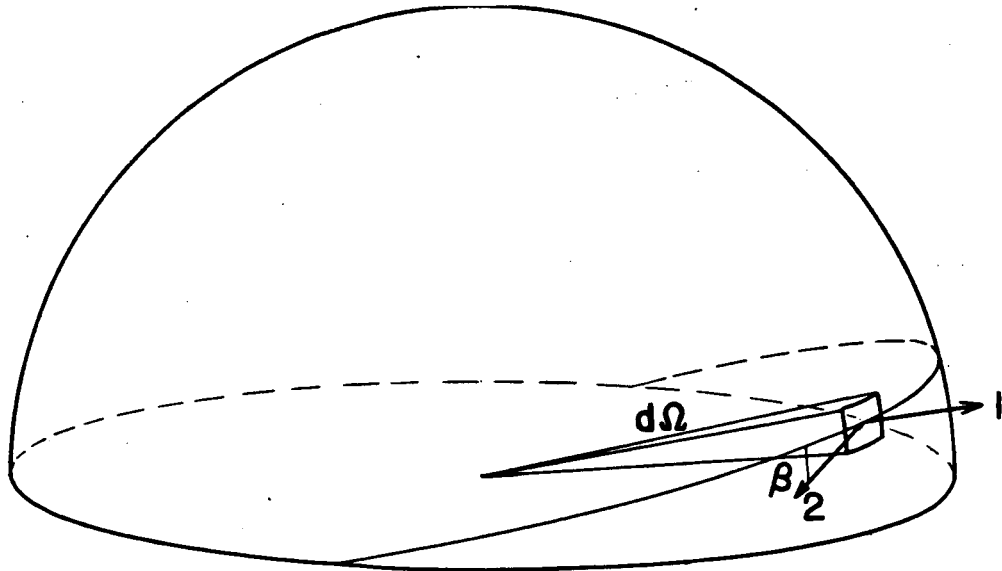


Figure 3.— Vectors normal to plane of slip and in direction of slip.

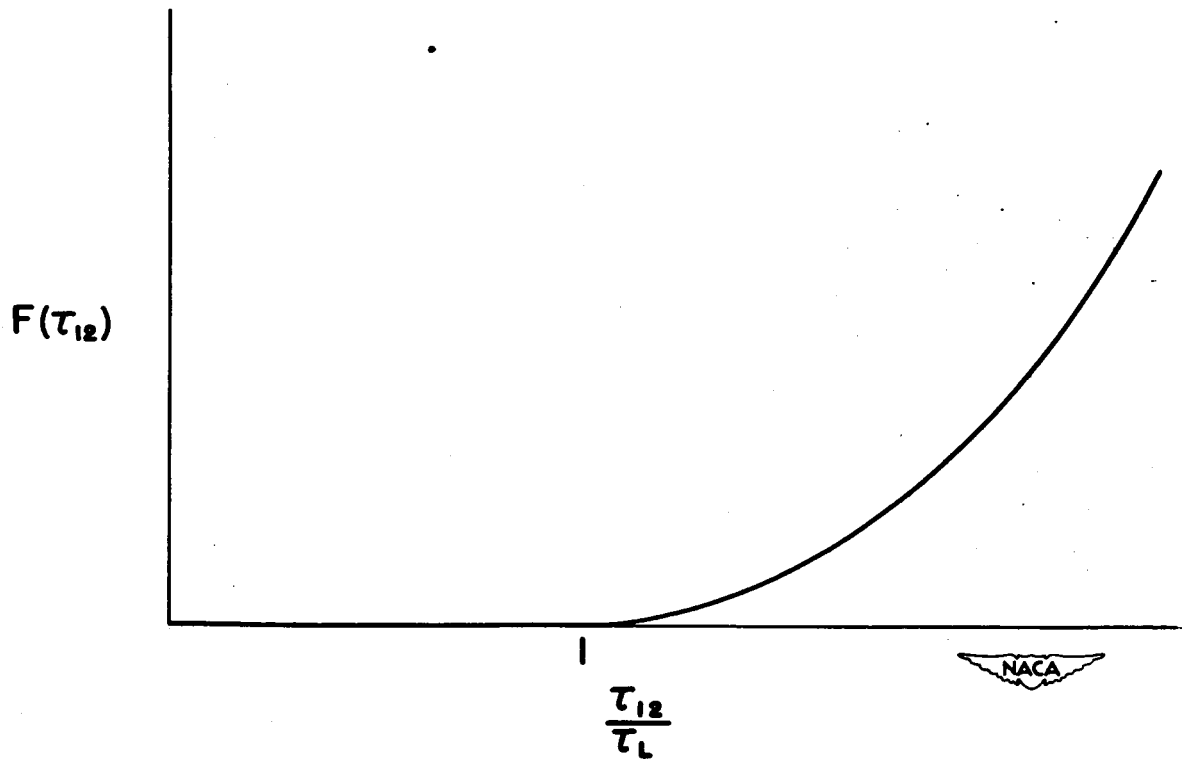


Figure 4.— Characteristic shear function (schematic).

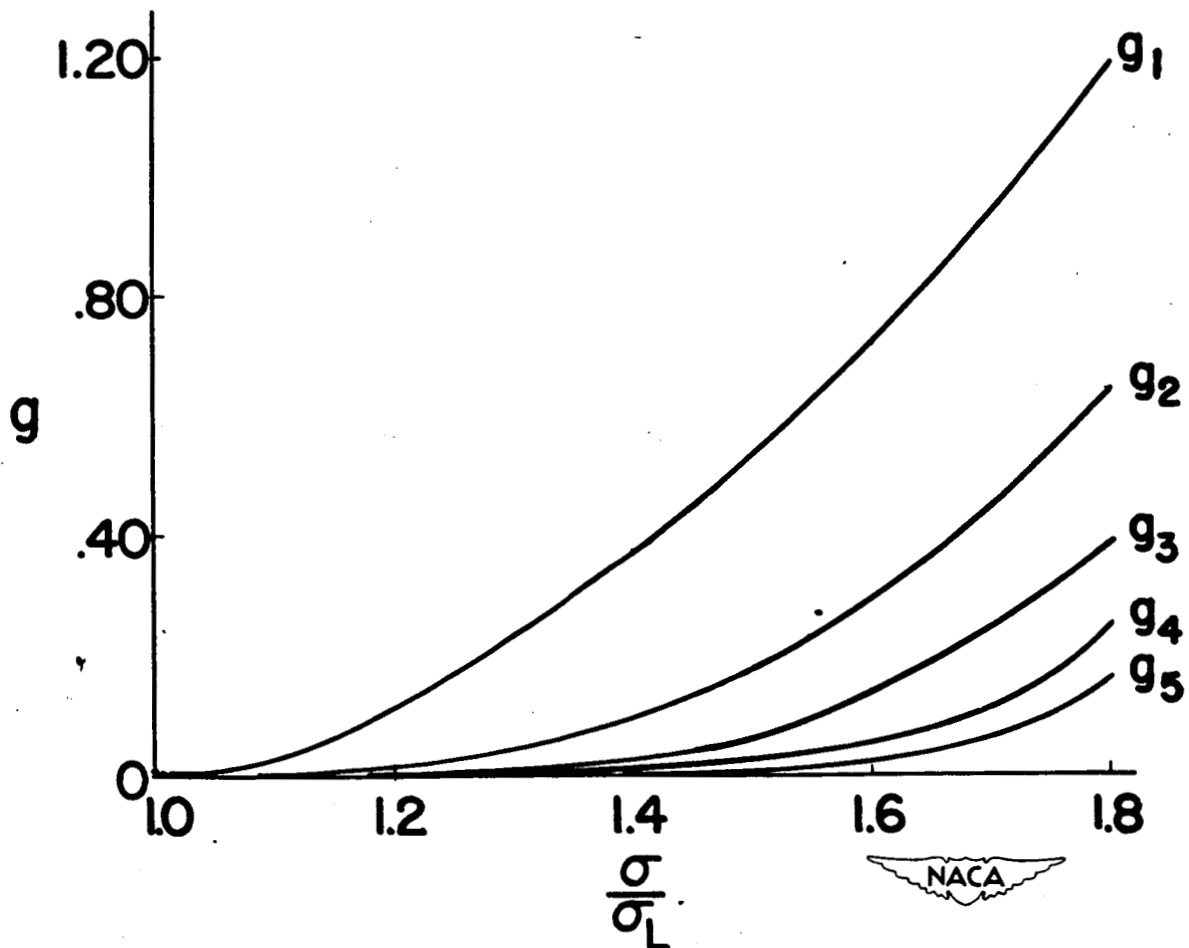


Figure 5.- Variations of tensile plastic strain with applied tensile stress corresponding to various terms in series expansion for characteristic shear curve.

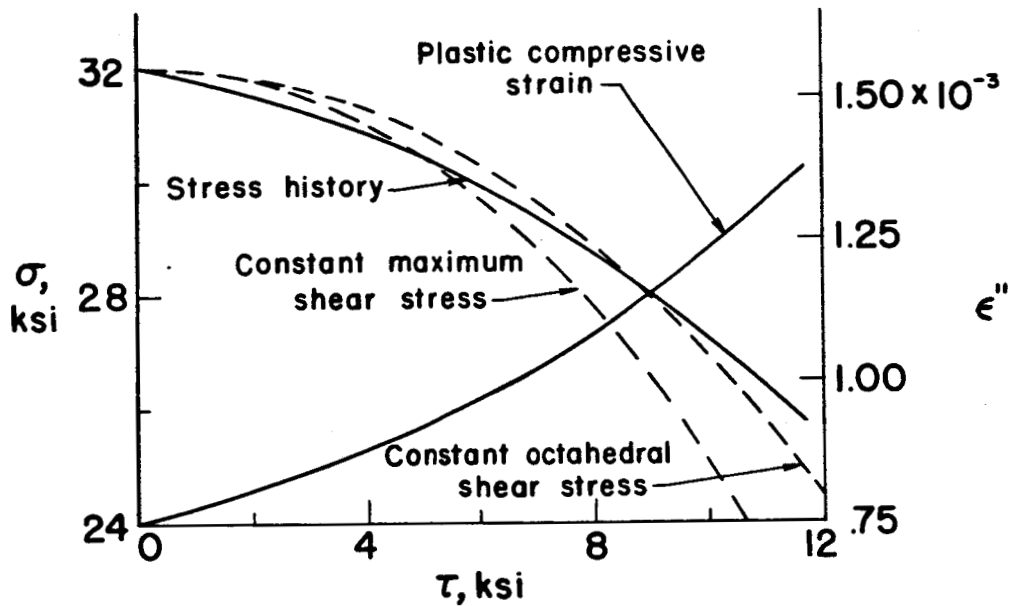


Figure 6.- Compressive stress and plastic compressive strain measured during twist of cylinder at constant total compressive strain.

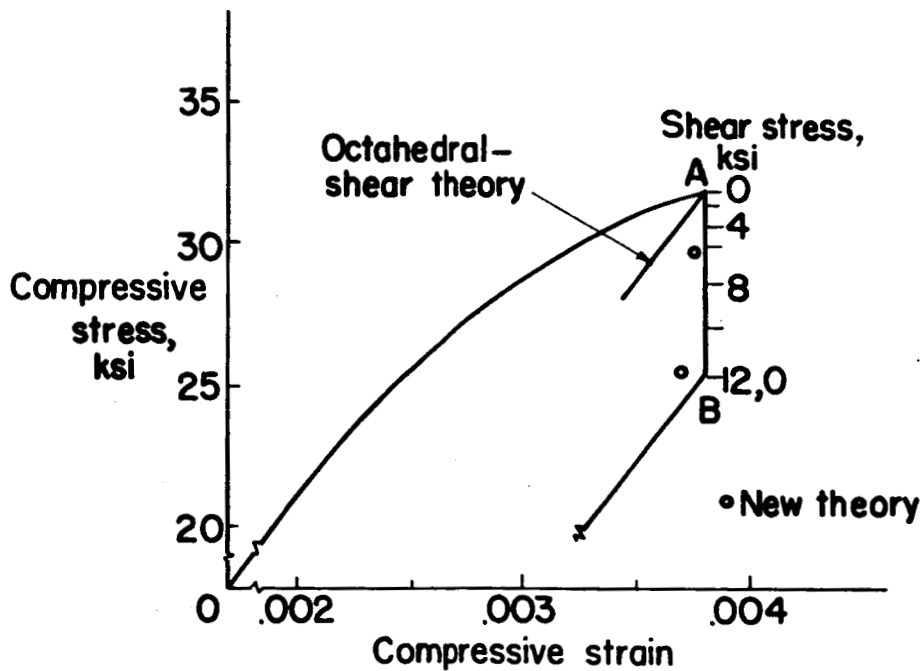


Figure 7.- Compressive stress-strain relations for cylinder subjected first to compression (OA), and then to torsion at constant compressive strain (AB), followed by removal of torsion and then compression.



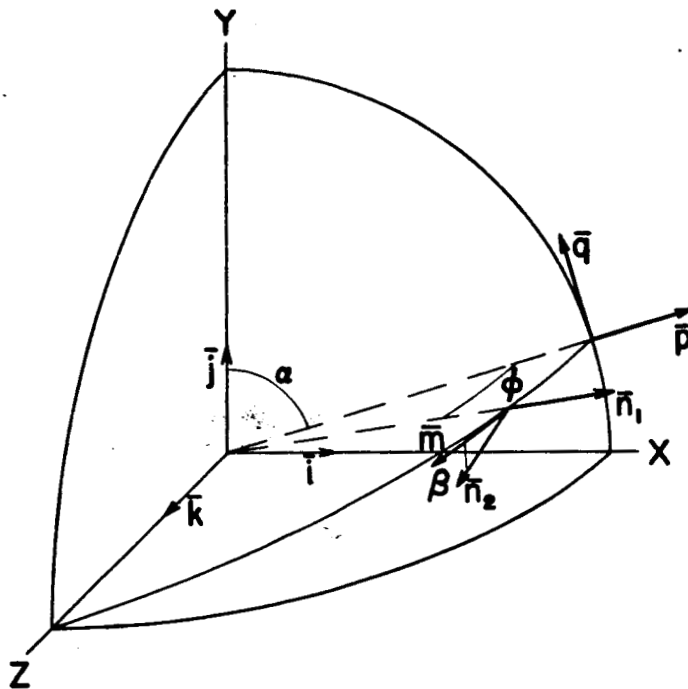


Figure 8.— Coordinate system used for analytical representation of direction cosines.

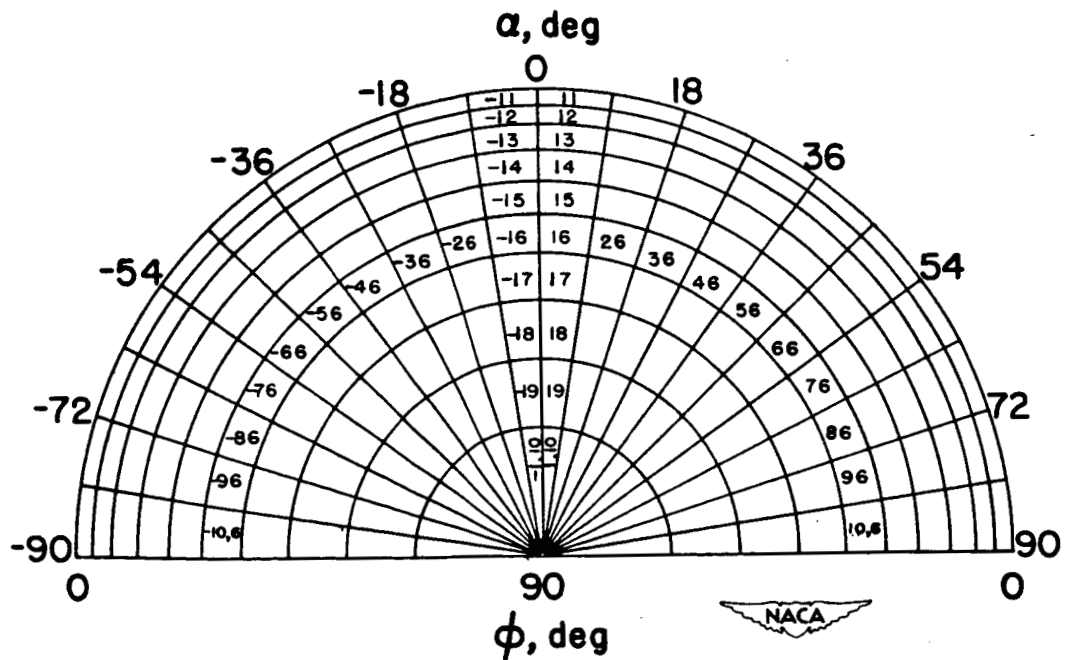
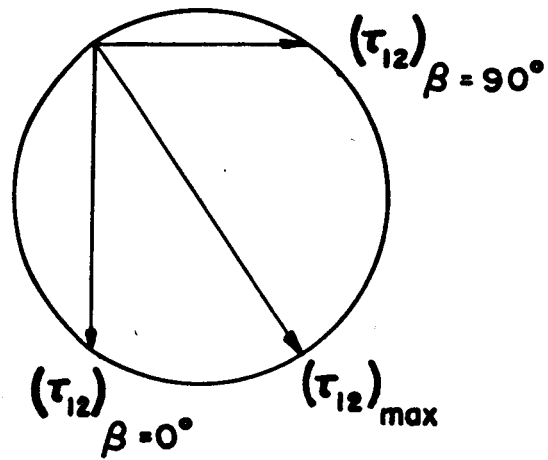
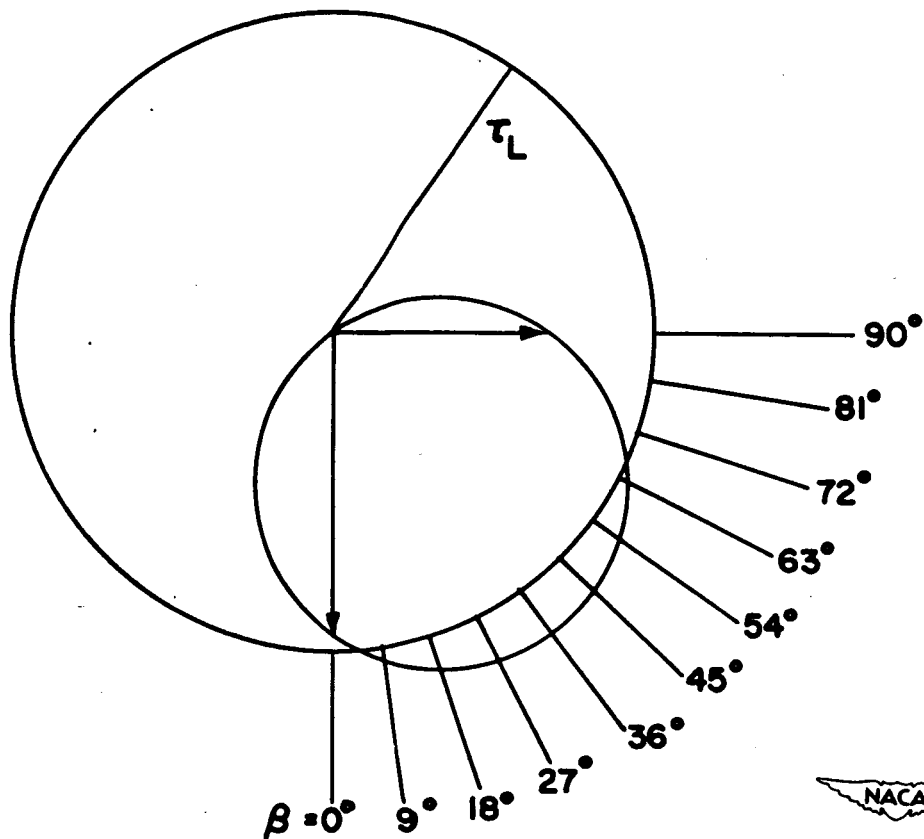


Figure 9.— System for classifying slip planes by means of plane orientation (schematic).



(a) Components of shear stress in various directions of slip.



(b) Slip directions are those in crescent.

Figure 10.-Graphical construction used in determining shear-stress components causing slip.

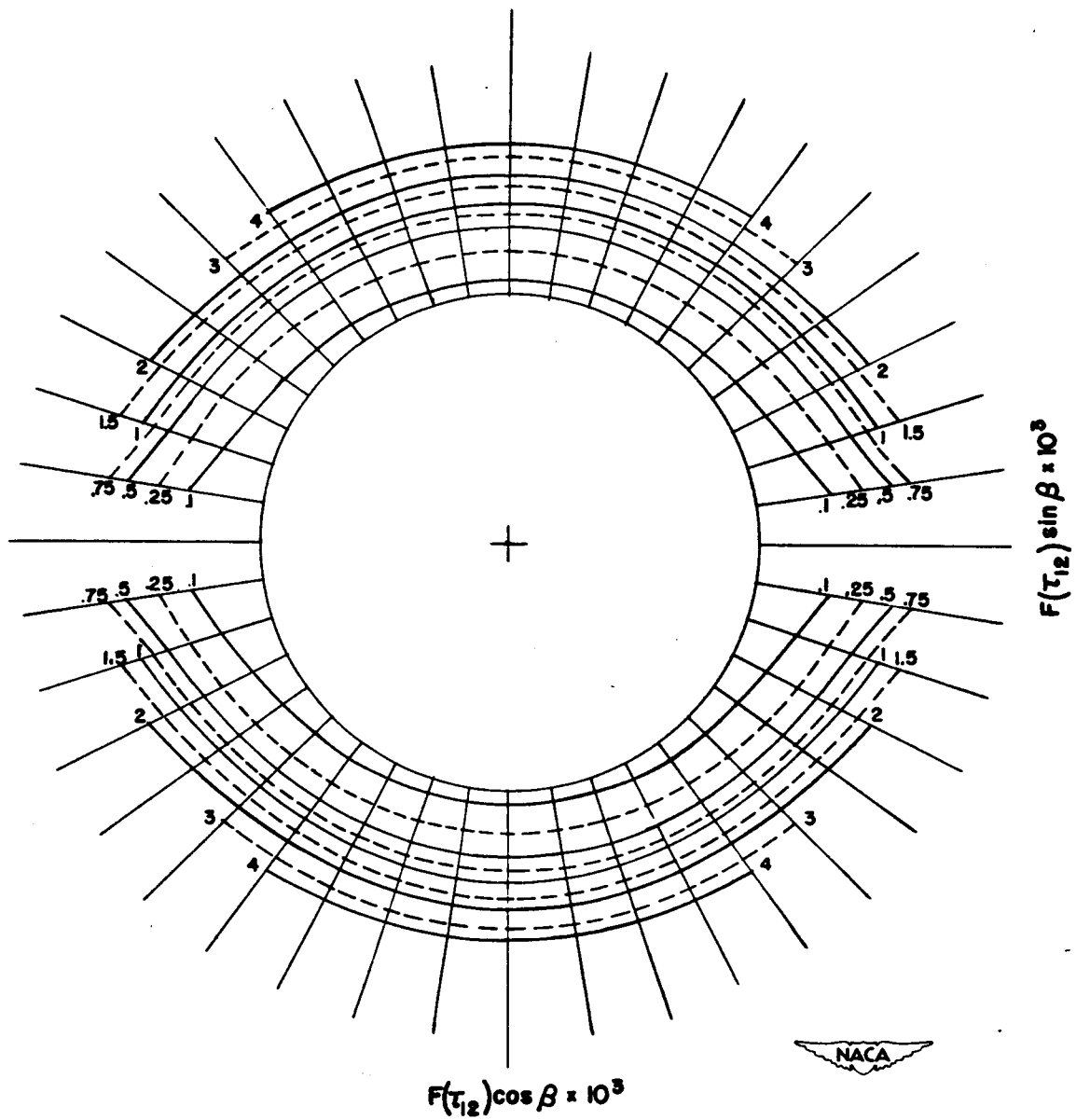


Figure 11.— Master chart for rapid evaluation of $F(\tau_{12})\cos\beta$ and $F(\tau_{12})\sin\beta$.

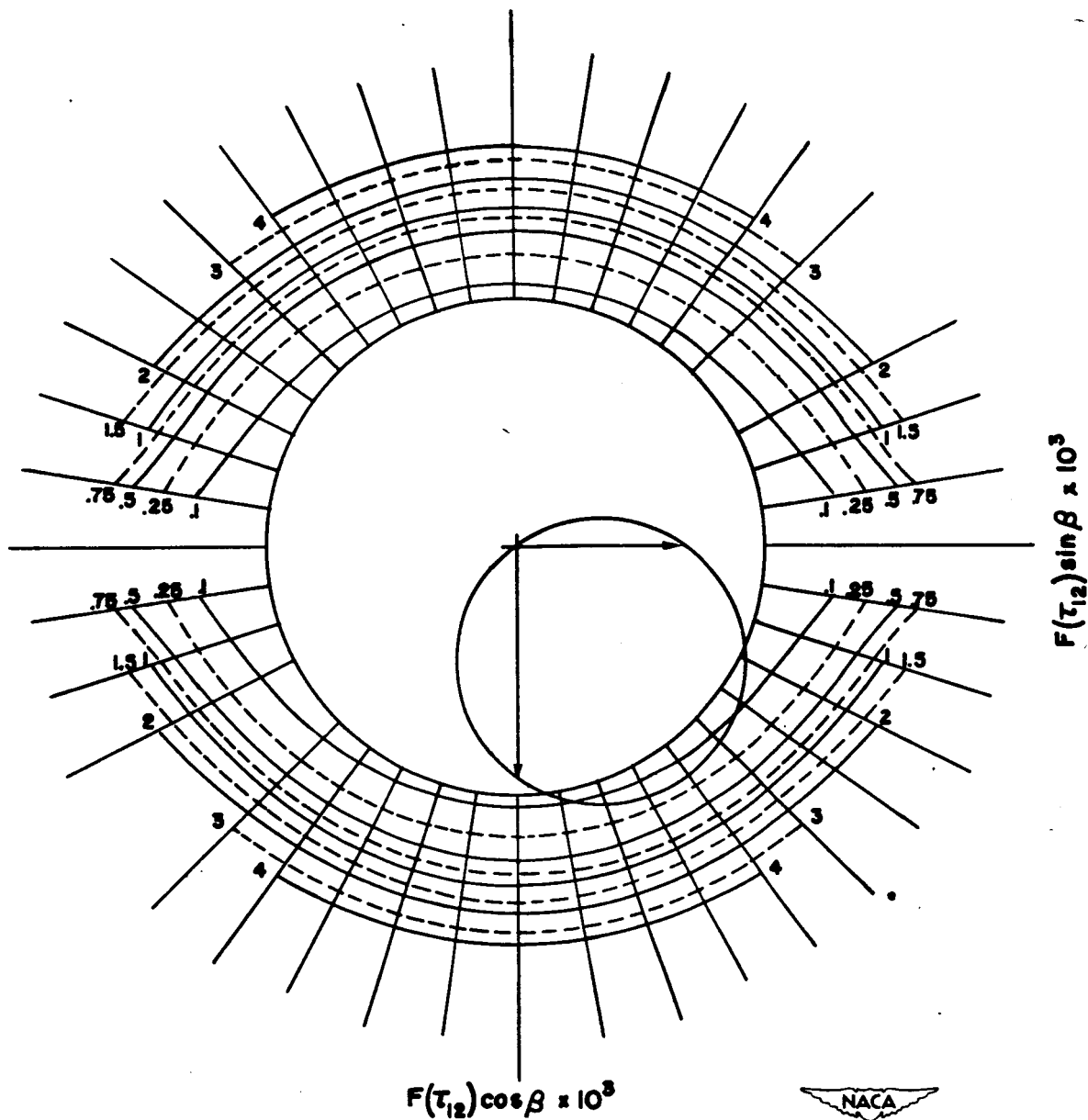


Figure 12.— Master chart fitted over shear-stress diagram (fig.10(a)) to permit direct reading of $F(\tau_{12})\cos\beta$.

Materials - Properties

5.2



A Mathematical Theory of Plasticity Based on the
Concept of Slip.

By S. B. Batdorf and Bernard Budiansky

NACA TN No. 1871
April 1949

(Abstract on Reverse Side)



Batdorf, S. B., and Budiansky, Bernard



A Mathematical Theory of Plasticity Based on the
Concept of Slip.

By S. B. Batdorf and Bernard Budiansky

NACA TN No. 1871
April 1949

(Abstract on Reverse Side)



Abstract

A new theory is proposed for the relationship between stress and strain for initially isotropic materials in the strain-hardening range. This theory is based on the assumption that slip in any direction along parallel planes of any particular orientation in the material gives rise to a plastic shear strain which depends only on the history of the corresponding component of shear stress. The theory is shown to give results in better agreement than previously existing theories with data obtained in a crucial type of experiment in which a cylinder was compressed into the plastic range and then twisted at constant compressive strain.

Abstract

A new theory is proposed for the relationship between stress and strain for initially isotropic materials in the strain-hardening range. This theory is based on the assumption that slip in any direction along parallel planes of any particular orientation in the material gives rise to a plastic shear strain which depends only on the history of the corresponding component of shear stress. The theory is shown to give results in better agreement than previously existing theories with data obtained in a crucial type of experiment in which a cylinder was compressed into the plastic range and then twisted at constant compressive strain.